Journal of Power Sources 273 (2015) 591–599

Contents lists available at ScienceDirect

Journal of Power Sources

journal homepage: www.elsevier.com/locate/jpowsour

$NdBaCo_{2/3}Fe_{2/3}Cu_{2/3}O_{5+\delta}$ double perovskite as a novel cathode material for CeO_2- and $LaGaO_3$-based solid oxide fuel cells

Fangjun Jin, Lei Li, Tianmin He*

Key Laboratory of Physics and Technology for Advanced Batteries, Ministry of Education, College of Physics, Jilin University, Changchun 130012, PR China

HIGHLIGHTS

- The structure and properties of NBCFC double perovskite are studied as IT-SOFC cathode.
- Introduction of Cu significantly reduces TEC and enhances oxygen vacancy concentration compared with NBCF material.
- NBCFC cathode exhibits good chemical compatibility and electrochemical performance with GDC and LSGM electrolytes.
- Addition of appropriate amounts of GDC to NBCFC further improves thermal expansion compatibility and electrochemical performance.

GRAPHICAL ABSTRACT

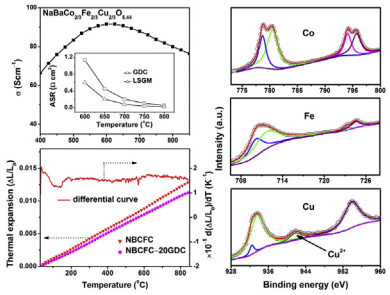

ARTICLE INFO

Article history:
Received 27 June 2014
Received in revised form
19 September 2014
Accepted 22 September 2014
Available online 2 October 2014

Keywords:
Solid oxide fuel cell
Double perovskite cathode
Chemical compatibility
Chemical state
Thermal expansion
Electrochemical performance

ABSTRACT

Double perovskites $LnBaCo_2O_{5+\delta}$ (Ln = rare earth) are explored as cathode materials for intermediate-temperature solid oxide fuel cell. Barriers to the applicability of double perovskite cathodes include high thermal expansion coefficient (TEC) and poor chemical compatibility with common electrolytes. In this paper, we report the characteristics and applicability of a double perovskite $NdBaCo_{2/3}Fe_{2/3}Cu_{2/3}O_{5+\delta}$ (NBCFC) cathode on CeO_2- and $LaGaO_3$-based electrolytes. NBCFC is found to crystallize in a tetragonal structure. Partial substitution of Fe and Cu for cobalt in NBCFC demonstrates significantly decreased TEC and good chemical compatibility with both $Gd_{0.1}Ce_{0.9}O_{1.95}$ (GDC) and $La_{0.9}Sr_{0.1}Ga_{0.8}Mg_{0.2}O_{3-\delta}$ (LSGM) electrolytes, while maintaining its good electrochemical performance. The oxidation states of transition metal cations are Co^{3+}/Co^{4+}, Fe^{3+}/Fe^{4+}, and Cu^{+}/Cu^{2+}, respectively. The average TEC of NBCFC is $15.7 \times 10^{-6}\ K^{-1}$ between 30 and 850 °C, and the polarization resistance values are 0.056 and 0.023 Ω cm^2 at 800 °C with GDC and LSGM electrolytes, respectively. The absence of spin-state transition in copper contributes to the TEC reduction. Addition of appropriate amounts of GDC into NBCFC to form NBCFC–GDC composite cathodes further reduce the TEC and improve cathode performance. These results can be used to improve and develop novel double perovskite cathode materials.

1. Introduction

Solid oxide fuel cells (SOFCs) are one of the most efficient electrochemical devices that convert chemical energy into usable electrical energy with high conversion efficiency and low levels of pollutants. Conventional SOFCs must operate at high temperature

* Corresponding author. Tel.: +86 431 85166112; fax: +86 431 85167827.
E-mail addresses: hetm@jlu.edu.cn, hly@mail.jlu.edu.cn (T. He).

http://dx.doi.org/10.1016/j.jpowsour.2014.09.147
0378-7753/

(typically at ~1000 °C) to obtain the required performance. This high operating temperature leads to degradation of fuel cell performance, interfacial reactions among the components, and limited choice of materials. Therefore, reducing the operating temperature of SOFCs from the traditional ~1000 °C to an intermediate temperature (IT) range of 600–800 °C is preferred (i.e., IT-SOFCs) [1,2]. Decreasing the operating temperature not only significantly prolongs the lifetime of the materials and reduces the SOFC system costs, but also provides broader material selection. However, the reduction in operating temperature of SOFCs results in larger polarization loss and slower oxygen reduction reaction kinetics than conventional cathode materials operated at high temperature. Therefore, developing a new cathode material with high electrochemical activity for oxygen reduction reaction in IT range is necessary to improve electrochemical performance.

Numerous mixed ionic and electronic conductors (MIECs) have been used as IT-SOFC cathode materials. Cobalt-based perovskite-type MIECs present more excellent electrocatalytic activity than those of conventional cathode materials, such as $La_xSr_{1-x}MnO_3$, in the IT range. In particular, double perovskite MIEC materials $LnBaCo_2O_{5+\delta}$ (Ln = rare earth) as cathodes for application in IT-SOFCs have received increased attention in recent years because of their distinct oxygen-deficient perovskite-related 112-type structure and stacking sequence of $\cdots CoO_x/LnO_\delta/CoO_x/BaO/CoO_x\cdots$. The oxygen vacancies in this compound are localized in the LnO_δ and CoO_x layers, and alternating ordered LnO_δ and BaO planes can improve oxygen transport as compared with ABO_3 perovskite oxides [3–6]. $LnBaCo_2O_{5+\delta}$ double perovskites have been used as IT-SOFC cathode materials because of their excellent electrocatalytic activity and mixed electronic–ionic conducting properties [4–10]. For example, Gu et al. [8] investigated the oxygen reduction reaction mechanism of $NdBaCo_2O_{5+\delta}$ (NBC) cathode with $Sm_{0.2}Ce_{0.8}O_{1.9}$ (SDC) electrolyte, which more easily showed oxygen diffusion processes. However, like cobalt-rich perovskite cathodes, NBC cathode exhibits a high thermal expansion coefficient (TEC), which can lead to lattice expansion and thermal expansion mismatch with SOFC components, thereby hampering their practical application. The high TEC values are related to low-spin to high-spin transitions of Co^{3+} ions, which can cause larger lattice expansion [11]. To decrease TEC values so as to obtain good thermal expansion compatibility with the most extensively used electrolyte materials, an effective method involves replacing cobalt ions with transition-metal ions such as Fe, Cu, and Ni [11–15] was established. Kim et al. [11,12] reported that the substitution of Fe and Cu for Co in $LnBaCo_{2-x}Cu_xO_{5+\delta}$ ($0 \le x \le 1.0$) and $NdBaCo_{2-x}Fe_xO_{5+\delta}$ led to decreased TEC. For example, average TEC values decreased from 20.7×10^{-6} K^{-1} for $NdBaCo_2O_{5+\delta}$ to 16.4×10^{-6} K^{-1} for $NdBaCoCuO_{5+\delta}$ between 80 and 900 °C. B-site co-doped $LnBaCo_2O_{5+\delta}$ have also been developed as a potential cathode for IT-SOFC applications. Kim et al. [15,16] reported that the Fe and Cu co-doped $SmBaCo_2O_{5+\delta}$ and $GdBaCo_2O_{5+\delta}$ exhibit decreased TEC, and the corresponding polarization resistances were 0.184 and 0.165 Ω cm^2 at 700 °C for $SmBaCo_{2/3}Fe_{2/3}Cu_{2/3}O_{5+\delta}$ (SBCFC) and $GdBaCo_{2/3}Fe_{2/3}Cu_{2/3}O_{5+\delta}$ (GBCFC) cathodes on $Gd_{0.1}Ce_{0.9}O_{1.95}$ (GDC) electrolyte. Zhou et al. [17] showed that Fe and Cu co-doping for Co in $GdBaCuCo_{0.5}Fe_{0.5}O_{5+\delta}$ displayed decreased TEC compared with that of the $GdBaCo_2O_{5+\delta}$ cathode, in which the average TEC value was 14.4×10^{-6} K^{-1} between 30 and 850 °C. Our group has also systemically investigated the performance of $PrBaCo_{2/3}Fe_{2/3}Cu_{2/3}O_{5+\delta}$ (PBCFC) double perovskite as IT-SOFC cathode material, which exhibits decreased TEC and excellent electrochemical performance [18]. Fe and Cu co-doping for Co results in decreased Co content, and thus reduces the effect of Co^{3+} spin transition on TEC. Moreover, the bonding energy of Fe–O is considerably higher than that of Co–O. Therefore, Fe doping for Co can also decrease TEC [11,19]. In addition, the substitution of transition-metal ions for Co in $LnBaCo_2O_{5+\delta}$ can further reduce the cost of cobalt-rich cathode material in SOFCs. Furthermore, compared with the two valence states of Pr^{3+} and Pr^{4+}, the single valence state of Nd^{3+} in perovskite oxides is beneficial for maintaining good chemical stability [20,21]. Therefore, to extend our work in this field, a double perovskite $NdBaCo_{2/3}Fe_{2/3}Cu_{2/3}O_{5+\delta}$ (NBCFC) was developed as novel cathode for use in IT-SOFCs. The effects of Fe and Cu co-doping in the cobalt site on the crystal structure, as well as the properties of the NBCFC material, were investigated in detail. The suitability and electrochemical performance of NBCFC cathode with CeO_2- and $LaGaO_3$-based electrolytes were assessed. The NBCFC double perovskite is a highly promising cathode material for application in IT-SOFCs.

2. Experimental

2.1. Sample preparation

$NdBaCo_{2/3}Fe_{2/3}Cu_{2/3}O_{5+\delta}$ (NBCFC) powders were prepared *via* an EDTA–citric acid complexation method. Stoichiometric amounts of Nd_2O_3 (Nd_2O_3 was dissolved in nitric acid to form a nitrate before use), $Ba(NO_3)_2$, $Co(NO_3)_2{\cdot}6H_2O$, $Fe(NO_3)_3{\cdot}9H_2O$, and $Cu(NO_3)_2{\cdot}3H_2O$ were mixed in deionized water as precursors. EDTA and citric acid were added as complexation agents. The molar ratio of total metal ions: EDTA: citric acid was 1:1:1.5. The pH value of the solution was adjusted by adding an appropriate amount of ammonia water. The mixed solution became transparent under heating and stirring conditions. A homogeneous black viscous gel was obtained after evaporating the excess water. The gel was dried in an oven at 180 °C for 4 h, and the dried powders were subsequently calcined at 400 °C for 6 h and 900 °C for 10 h. The calcined powders were pelletized by uniaxial mold pressing powders at 220 MPa and then sintered at 950 °C for 10 h in air to obtain the final composition with the required NBCFC phase. $Ce_{0.8}Sm_{0.2}O_{1.9}$ (SDC), $Ce_{0.9}Gd_{0.1}O_{1.95}$ (GDC), $La_{0.9}Sr_{0.1}Ga_{0.8}Mg_{0.2}O_{3-\delta}$ (LSGM), and NiO powders were prepared by the glycine–nitrate process [22]. The composite cathodes were prepared by introducing 10 and 20 wt.% GDC into pure NBCFC cathode, fully ground with an agate mortar for 2 h, and noted as NBCFC–10GDC and NBCFC–20GDC, respectively. Dense CeO_2-based and LSGM electrolytes were obtained by sintering the samples at 1400 °C for 10 h and 1450 °C for 10 h, respectively. Well-mixed NiO and GDC powders (65:35 weight ratio) were used as anode material.

2.2. Material characterization

The phase structure of the prepared cathode and chemical compatibility with electrolytes were identified by X-ray diffraction (XRD, Rigaku D/Max-2550) using Cu K_α radiation ($\lambda = 0.15418$ nm) at room temperature with a 0.02° step size. The surface microstructure and chemical composition of the NBCFC sample were inspected using scanning electron microscopy (SEM, JEOL JSM-6480LV) and energy-dispersive X-ray spectroscopy (EDS, EDAX). XPS analyses were performed on an X-ray photoelectron spectrometer (VG Scientific ESCALAB MK II). The measurements were obtained with a monochromatized, microfocused Al Kα (1486.6 eV) radiation source. Detailed measurements and analyses were described in our previous work [18]. The TEC of the sample was measured by a dilatometer (Netzsch DIL 402C) in the temperature range of 30 °C–850 °C. The air-purge flow rate was controlled at 60 mL min^{-1}. Oxygen content ($5 + \delta$) was determined by iodometric titration technique. Thermogravimetric analysis (TGA) was

carried out using a thermal analyzer (HCT-3 HENVEN) at a flow rate of 50 mL min^{-1} air and operated from 30 °C to 900 °C at a heating rate of 10 °C min^{-1}. The electrical conductivities of the NBCFC sample were measured using van der Pauw method between 300 and 850 °C in air. Electrochemical performance measurements were conducted with an electrochemical analyzer (CHI604D, Chenhua). Impedance spectra were recorded in a frequency range of 0.1 Hz−1 × 10^5 Hz under open circuit conditions, and the signal amplitude was 10 mV.

2.3. Cell fabrication and test

Electrolyte (thickness: 0.3 mm)-supported symmetric and single cells were fabricated by screen printing method. For symmetric cells, the cathode slurry was painted on both sides of the GDC and LSGM substrates, and then sintered at 950 °C for 2 h. Silver paste was used as current collector on the cathodes. Symmetric cells were measured in air at 600 °C–800 °C in 50 °C intervals. For the single cell with LSGM electrolyte, a GDC buffer was used to prevent chemical reaction between Ni and LSGM electrolyte in high temperature. The GDC slurry was screen-painted on the sides of LSGM pellets to form an interlayer and was then sintered at 1300 °C for 1 h. The anode was painted onto the GDC interlayer and then sintered at 1250 °C for 4 h. Similarly, the cathode was painted onto the opposite side of the GDC and LSGM electrolytes and sintered at 950 °C for 2 h. The single cell was sealed onto one end of an alumina tube using silver paste as a sealant. Single cell performance was recorded under dry hydrogen and ambient air measured between 600 and 800 °C.

3. Results and discussion

3.1. Crystal structure and chemical compatibility

Fig. 1(a) shows the XRD pattern of the NBCFC sample sintered at 950 °C for 10 h in air. For the purpose of comparison, the XRD patterns of $NdBaCoFeO_{5+\delta}$ (NBCF) [21] and $NdBaCo_2O_{5+\delta}$ (NBC) materials are also included in Fig. 1(a). A single-phase NBCFC double perovskite is obtained after sintering at 950 °C for 10 h. All diffraction peaks of the sample can be indexed in a tetragonal structure with the space group P4/*mmm*. This result is demonstrated by the tetragonal structure characteristics of double perovskite, as shown in the inset of Fig. 1(a), where XRD peak splitting occurs at the (110), (102), (212), and (114) planes [18]. The XRD diffraction peaks of NBCFC shift toward lower 2θ values compared with those of NBC and NBCF. Given that Fe and Cu have substantially larger ionic radii than that of Co [23], these ions cause an increased unit cell volume, thereby resulting in a shift of the diffraction peaks from a higher to a lower angle. The calculated unit cell parameters of NBC and NBCF are listed in Table 1.

Rietveld refinement was performed on the NBCFC sample with the FullProf program and shown in Fig. 1(b). This method reveals that all reflection can be indexed to a tetragonal phase of the NBCFC crystal with refined lattice parameters as given in Table 1. The reasonable values of *R* factors ($R_{wp} = 6.43$, $R_p = 5.91$, and $\chi^2 = 2.26$) confirm good refinement in tetragonal structure.

To assess the chemical compatibility of NBCFC with the most common IT-SOFC electrolytes (SDC, GDC, and LSGM), NBCFC oxide and the electrolytes in a 1:1 weight ratio were mixed, followed by

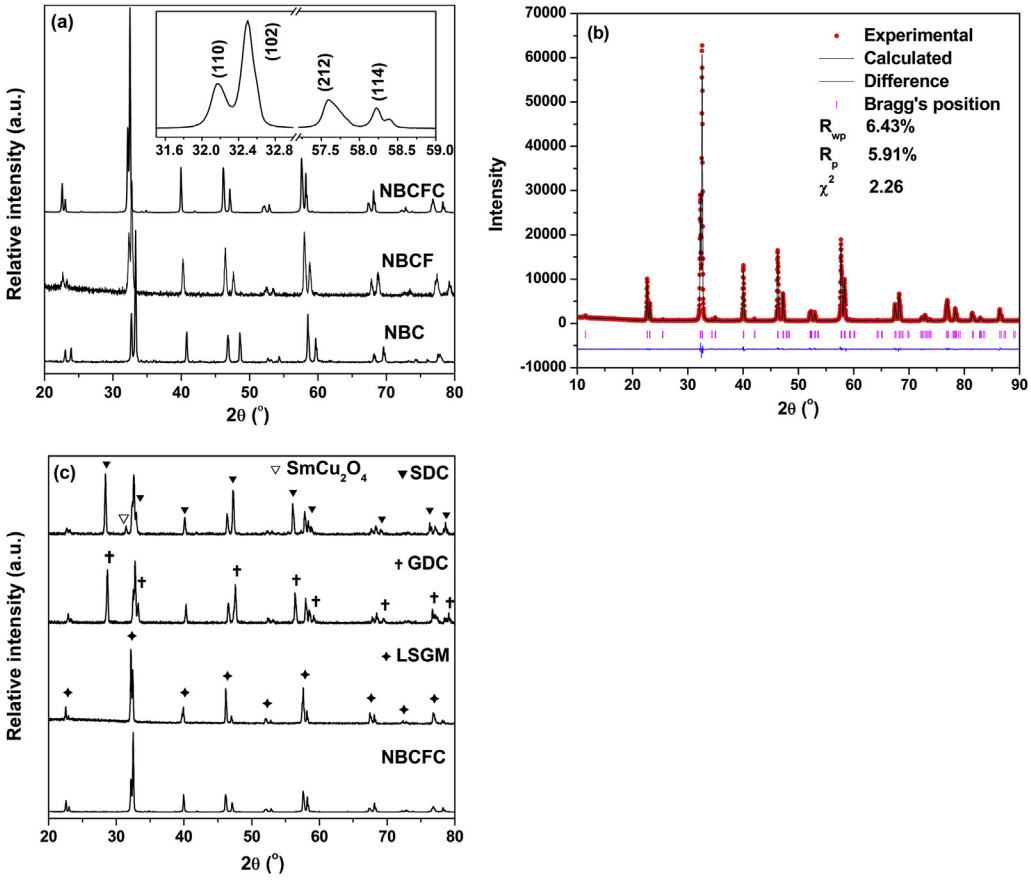

Fig. 1. (a) XRD patterns of samples NBCFC and NBCF [21], as well as NBC; (b) Rietveld refined XRD pattern for NBCFC: the atomic positions are Nd (0, 0, 0), Ba (0, 0, 1/2), (Co, Fe, and Cu) (0.5, 0.5, 0.2401(3)), O1 (1/2, 1/2, 0), O2 (1/2, 1/2, 1/2), and O3 (1/2, 0, 0.2037(4)); (c) XRD patterns of NBCFC–SDC, NBCFC–GDC, and NBCFC–LSGM mixtures calcined at 950 °C for 10 h in air.

Table 1
Unit cell parameters, oxygen content, oxidation states, and TECs of NBC [5,6], NBCF [21], and NBCFC samples.

Sample	Unit cell parameters			Oxygen content ($5+\delta$)	Oxidation state of (co, Fe, Cu)	TEC ($\times 10^{-6}$ K^{-1})
	a (nm)	c (nm)	V (nm3)			
NBC	0.3878(8)	0.7699(0)	0.1158(3)	5.78	3.28	20.0
NBCF	0.3909(0)	0.7625(2)	0.1165(2)	5.67	3.17	19.5
NBCFC	0.3923(1)	0.7696(4)	0.1185(1)	5.44	2.94	15.7

Table 2
EDS results of the NBCFC sample.

Metal elements		wt.%	At.%	Elemental ratio (EDS results)	Elemental ratio (nominal values)
A-site	Nd	27.0	9.3	0.964	1.000
	Ba	27.9	10.0	1.036	1.000
B-site	Co	7.5	6.3	1.011	1.000
	Fe	7.1	6.3	1.011	1.000
	Cu	7.7	6.1	0.978	1.000

calcining at 950 °C for 10 h in air. Fig. 1(c) shows the XRD patterns of NBCFC and the electrolyte mixtures after heat treatment. A new diffraction peak corresponding to $SmCu_2O_4$ (JCPDS #87–1744) is evidently observed in the NBCFC–SDC mixture. This result indicates that NBCFC reacts with the SDC electrolyte after calcination, thereby suggesting that NBCFC is not chemically compatible with SDC electrolyte at 950 °C. However, no impurity phases or diffraction peak shifts are observed in the NBCFC–GDC and NBCFC–LSGM mixtures, indicating that NBCFC presents good chemical compatibility with GDC and LSGM electrolytes at temperatures up to 950 °C. These results suggest that NBCFC presents chemical stability as cathode for applications in IT-SOFCs based on GDC and LSGM electrolytes below 950 °C.

3.2. SEM and EDS analyses

Fig. 2(a) and (b) show the SEM micrograph and EDS spectra of the NBCFC sample sintered at 950 °C for 10 h. As seen from Fig. 2(a), a dense NBCFC sample was obtained after sintering at 950 °C for 10 h. The NBCFC sample is composed of homogeneous particles with an average grain size of 2 μm–3 μm. As can be seen from Fig. 2(b), only six elements, namely, Nd, Ba, Co, Fe, Cu, and O, exist in the sample. The EDS results are presented in Table 2. The actual measurements of the metal elements are in good agreement with the nominal composition of the NBCFC material. The XRD, SEM, and EDS results show that we obtain a dense and near-stoichiometric NBCFC by sintering the sample at 950 °C for 10 h, thus showing the suitable sintering condition.

3.3. XPS

XPS was used to investigate the oxidation states of transition metal cations in the NBCFC sample. Fig. 3 presents Co 2p, Fe 2p, and Cu 2p XPS spectra of NBCFC with a 2p doublet line ($2p_{3/2}$ and $2p_{1/2}$). As shown in Fig. 3(a), the Co $2p_{3/2}$ and $2p_{1/2}$ core level spectra are deconvoluted in peaks at binding energy of 778.7 and 794.1 eV for Co^{3+} and 780.5 and 795.7 eV for Co^{4+}, which are consistent with those reported in literature [18,21]. Deconvoluted Fe ($2p_{3/2}$ and $2p_{1/2}$) core level spectra are shown in Fig. 3(b), in which the peaks at 710.1 eV in $2p_{3/2}$ and 723.2 eV in $2p_{1/2}$ are assigned to Fe^{3+}, and 711.7 eV in $2p_{3/2}$ and 724.5 eV in $2p_{1/2}$ are representative of Fe^{4+}. Similar results have been reported in previous studies [18,21,24]. Fig. 3(c) shows the XPS results of Cu 2p core level spectra at $2p_{3/2}$ and $2p_{1/2}$ of the NBCFC sample. The binding energies for the Cu $2p_{3/2}$ peak of the Cu^+ and Cu^{2+} are 932.4 and 933.6 eV, respectively. The satellite peak at around 941.8 eV can be assigned to the Cu^{2+} species [25,26]. The peak area measurements show that the total Cu^{2+} peak area is considerably larger than the Cu^+ peak area, which indicate that the domination of Cu^{2+} state is over Cu^+ state in the NBCFC material.

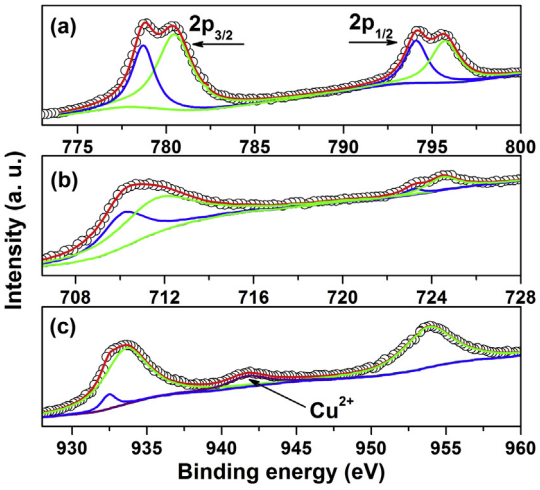

Fig. 3. XPS spectra (open circles) and fitted lines of the NBCFC sample at room temperature: (a) Co 2p, (b) Fe 2p, and (c) Cu 2p.

XPS analyses reveal that the Co^{3+}/Co^{4+}, Fe^{3+}/Fe^{4+}, and Cu^+/Cu^{2+} cations coexist in NBCFC. Interestingly, no spin-state transitions exist in Cu^+/Cu^{2+} cations, indicating that the absence of spin-state transition of Cu^+/Cu^{2+} contributes to the reduction in the TEC of NBCFC. The mixed valences favor the redox cycles of the cathode

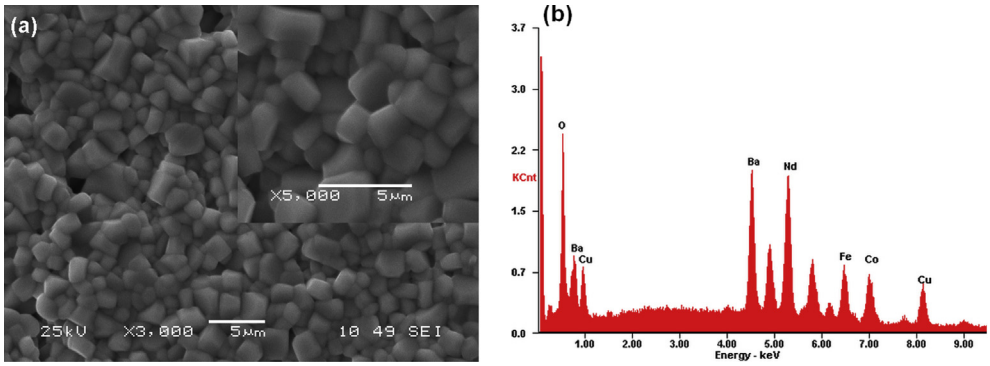

Fig. 2. (a) SEM micrograph and (b) EDS spectra of the NBCFC sample sintered at 950 °C for 10 h.

Table 3
Binding energies and percentage contributions of core electrons of NBCFC and NBCF.[21].

Sample	Co $2p_{3/2}$		Fe $2p_{3/2}$		Cu $2p_{3/2}$	
	Co^{3+} (%)	Co^{4+} (%)	Fe^{3+} (%)	Fe^{4+} (%)	Cu^{+} (%)	Cu^{2+} (%)
NBCF	778.4 (29.1%)	780.4 (70.9%)	709.7 (40.1%)	711.4 (59.9%)	–	–
NBCFC	778.7 (34.0%)	780.5 (66.0%)	710.1 (34.6%)	711.7 (65.4%)	732.4 (4.2%)	733.6 (95.8%)

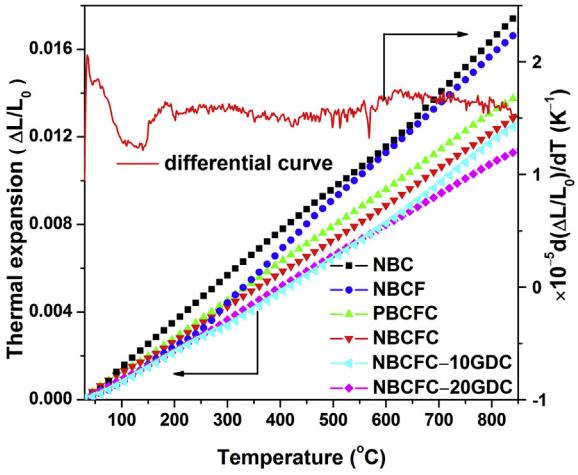

Fig. 4. Thermal expansion curves of NBC, NBCF [21], PBCFC [18], and NBCFC samples between 30 and 850 °C in air.

through enhancing the mobile active oxygen in the crystal structure. Table 3 gives the binding energies and percentage contributions of core electrons of NBCF and NBCFC. We can see that the introduction of low-valence Cu^{+}/Cu^{2+} changes the Co^{4+}/Co^{3+} and Fe^{4+}/Fe^{3+} ratios compared with NBCF [21], but no change in the oxidation state of Co and Fe cations was observed, which means that the oxygen vacancy concentration in this compound has changed. As demonstrated by iodometric titration measurements (Table 1), the oxygen content of NBCFC and NBCF samples are 5.44 and 5.67 [18] at room temperature, respectively. This finding indicates that the introduction of low-valence Cu significantly increases oxygen vacancy concentration. A similar result has been observed for NBCF [18], in which the introduction of Fe resulted in an increase in the number of oxygen vacancies from 0.22 for NBC [6] to 0.33 for NBCF [18]. These oxygen vacancies would further enhance oxygen permeation property and oxygen ion conductivity. Therefore, the mixed valence Co^{3+}/Co^{4+}, Fe^{3+}/Fe^{4+}, and Cu^{+}/Cu^{2+} cations tend to improve the oxygen ion conductivity and electrochemical performance of the NBCFC cathode [18].

3.4. Thermal expansion behavior and TGA

Good thermal expansion compatibility between cathode and electrolyte materials is crucial to ensure long-term operational stability and minimize the internal thermal stress of SOFC systems. Fig. 4 shows the thermal expansion curves of NBC, NBCF [21], and NBCFC samples measured between 30 and 850 °C in air, and the differential curve of NBCFC is also included in Fig. 4. The thermal expansion curve of the NBCFC sample appears linear in the measured temperature range. No sudden changes occur in the TEC curve of the NBCFC sample, which implies that no structural phase transition occurs in the IT-SOFC operating temperature range. As shown in Fig. 4 and Table 1, the NBCFC sample exhibits the lowest TEC value of 15.7×10^{-6} K^{-1}, which is lower than that of NBC, NBCF, and PBCFC [5,18,21]. Kim et al. [15,16] demonstrated that Fe and Cu co-doping for Co could effectively reduce the TEC of SBCFC and GBCFC, which were 16.6×10^{-6} and 14.6×10^{-6} K^{-1} between 30 and 900 °C, respectively. The low-spin to high-spin transition of Co^{3+} ions is generally considered to be the main causes for the high TEC of cobalt-containing perovskite cathodes [27]. Fe and Cu co-doping for Co sites in NBC decreases the content of Co^{3+} ions from low-spin to high-spin transition, thus leading to decreased TEC. In addition, Fe–O bond strengths are larger than that of Co–O [19,28]. Therefore, the substitution of Fe for Co causes a decrease in TEC. Moreover, the more covalent Cu–O bond compared with Co–O bond also contributes to a reduction in TEC [11]. The TEC of NBCFC sample is lower than that of NBCF, which is mainly due to the fact that the absence of spin-state transition in copper contributes to a reduction in TEC for NBCFC.

To reduce TEC further, NBCFC–10 wt.% GDC (NBCFC–10GDC) and NBCFC–20 wt.% GDC (NBCFC–20GDC) composite cathodes were prepared. As expected, the introduction of GDC electrolyte effectively reduces the TEC value of NBCFC–GDC composite cathodes (Fig. 4). The TEC value of the NBCFC–20GDC composite cathode decreases to 14.0×10^{-6} K^{-1} between 30 and 850 °C. The reduction in the TEC of the NBCFC–GDC composite cathode is attributed to the lower TEC of the GDC electrolyte (~12.0×10^{-6} K^{-1}).

Fig. 5 shows the variations of the oxygen content and oxidation state of (Co, Fe) in the NBCFC sample with temperature in flowing air. For comparison, the corresponding data for NBCF [21] are also included in Fig. 5. The oxygen non-stoichiometric value was determined by iodometric titration at room temperature. Evidently,

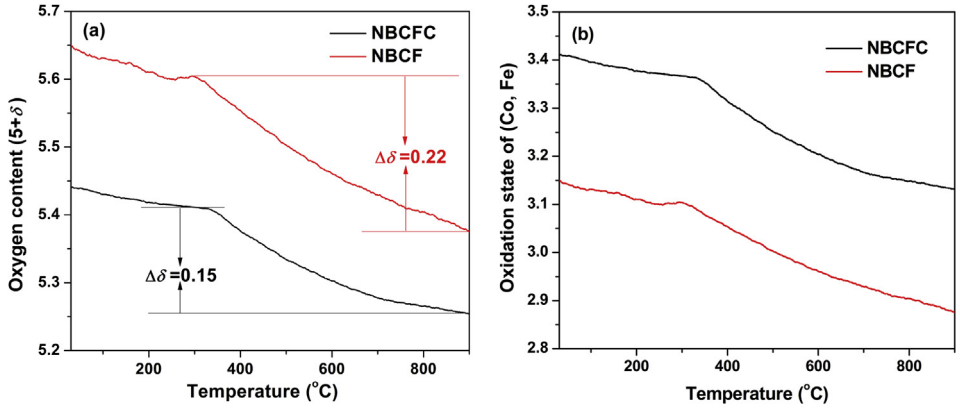

Fig. 5. (a) Variations in oxygen content and (b) the oxidation state of (Co, Fe) in NBCFC and NBCF [21] samples with temperature in air. Cu is assumed to exist as Cu^{2+} in (b).

strong oxygen loss starts at $T > 300$ °C, which corresponds to the loss of oxygen from the lattice due to weakly bonded O atoms in the sample. Meanwhile, transition metal cations are reduced from high oxidation state to low oxidation state with increasing temperature [29,30]. The oxygen content values of NBCFC and NBCF samples are 5.44 and 5.67 [18] at room temperature, respectively. The oxygen content value of NBCFC is lower than that of the NBCF sample because of the introduction of low-valence Cu, which decreases the average oxidation state of cations at the B-site. However, the oxygen content change value in NBCFC ($\Delta\delta = 0.15$) is lower than that in NBCF ($\Delta\delta = 0.22$) in the 300 °C–900 °C temperature range. Moreover, according to TGA results [Fig. 5(b)], the average oxidation state of (Co, Fe) in the NBCF and NBCFC samples (assuming that Cu exists as Cu^{2+}) is +2.88 and +3.13 at 900 °C, respectively. These results indicate that the introduction of Cu in NBCFC inhibits the thermal reduction of Co and Fe cations, and thus, considerably improves the phase stability at temperatures above 300 °C.

3.5. Electrical conductivity

Fig. 6(a) shows the electrical conductivity of NBCFC measured at different temperatures in air. For comparison, the electrical conductivity data of NBCF [21] are also included in Fig. 6(a). As a MIEC, total conductivities include both electronic and oxygen ionic conductivities. Electronic conductivity is significantly greater than oxygen ionic conductivity. Therefore, conductivity measured in the sample mainly referred to electronic conductivity. The NBCFC sample presents a semiconductor conduction behavior up to 625 °C and then changes into metallic-like conduction behavior in the subsequent temperatures. Electrical conductivity reaches a maximum value of 92 S cm^{-1} at 625 °C. This variation tendency is similar to those of the NBC and NBCF samples [11,21]. However, the conductivity values of NBCFC are lower than those of previously reported NBC and NBCF samples [11,21]. The reduction of conductivity in NBCFC can be interpreted in terms of the changes in charge carrier and oxygen vacancy. The conductivity mechanism in the $LnBa(Co, Fe, Cu)_2O_{5+\delta}$ materials is believed to be hopping of *p*-type small polarons [4,31], in which the holes are the major carriers. The Co^{4+} cations are the charge carriers (hole conduction) in the NBCFC material. As shown in Table 3, the concentration of Co^{4+} cations in NBCFC decreases relative to that of NBCF [21], thereby reducing electrical conductivity in NBCFC. As discussed in Section 3.3, oxygen vacancy concentration increases with the introduction of low-valence Cu. The increased oxygen vacancies in NBCFC also decrease conductivities. Electronic conduction in NBCFC proceeds *via* electron hopping along the Co^{4+}–O^{2-}–Co^{3+} bonds, and the creation of oxygen vacancies impedes the electron hopping pathway along the Co^{4+}–O^{2-}–Co^{3+}, thereby resulting in a decrease in electrical conductivities [32,33]. Notably, the introduction of Cu in NBCFC shifts the onset of semiconductor–metal transition temperature toward higher temperatures compared with NBCF. This result is mainly because the introduction of Cu can inhibit the thermal reduction of Co and Fe cations and improve the phase stability above 300 °C. This fact has been demonstrated by the TGA data in Section 3.4. The increase in the electrical conductivity of NBCFC below 625 °C can be attributed to the increase in charge carrier mobilities induced by thermal activation, whereas the decrease in electrical conductivity above 625 °C is due to oxygen loss from the lattice and the formation of oxygen vacancy. As demonstrated by the TGA data in Fig. 5, oxygen vacancy concentration increases with increasing temperature. The increased oxygen vacancies decrease the charge carrier concentration of the NBCFC sample, resulting in a decrease in electrical conductivity with temperature. The electrical conductivity value of NBCFC is higher than those of other double perovskite cathodes, such as $GdBaCuCo_{0.5}Fe_{0.5}O_{5+\delta}$ [17] and $GdBaCuCoO_{5+\delta}$ [34]. The electrical conductivity values ranging between 92 and 80 S cm^{-1} in the 600–800 °C temperature range are still highly advantageous for use as cathode for IT-SOFCs.

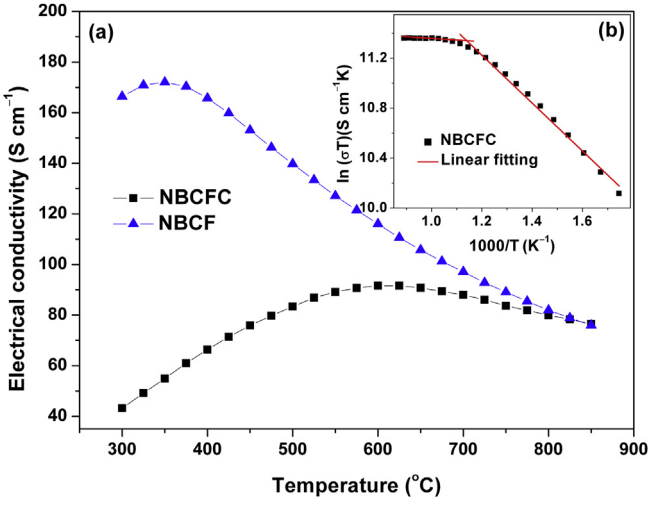

Fig. 6. (a) Temperature dependence of electrical conductivity for NBCFC and NBCF [21] samples and (b) Arrhenius plots of electrical conductivity for NBCFC sample.

Fig. 6(b) shows the Arrhenius plot of conductivity for the NBCFC sample. For a small polaron conduction mechanism [33], the activation energy can be expressed by the Arrhenius Eq. (1):

$$\sigma = \frac{A}{T}\exp\left(\frac{-Ea}{KT}\right) \quad (1)$$

where A is the pre-exponential factor, T is the absolute temperature, Ea is the activation energy, and K is the Boltzmann constant. The activation energies calculated from the slope of the fitted line in the $\ln(\sigma T)$ *vs* $1000/T^{-1}$ curve are 16.0 and 0.9 kJ mol^{-1} in the low and high temperature ranges, respectively.

3.6. Impedance spectroscopy

Fig. 7(a) and (b) show the typical impedance spectra of NBCFC on GDC and LSGM electrolytes measured at 600 °C–800 °C in air, respectively. The different electrode processes for oxygen reduction are characterized by two depressed arcs. The left intercept of the impedance spectrum on the real axis is the ohmic resistance of the cell, which includes the electrolyte, electrodes, current collectors, and lead wires. The right intercept is the total resistance of the cell. Therefore, the difference between the right and left intercepts on the real axis represents the total cathode–electrolyte interfacial resistance (area specific resistance, ASR). For a MIEC cathode material, the high-frequency arc (left arc) reflects charge transfer, including electron transfer and ion transfer at the interface of the current collector/electrode and electrode/electrolyte. This process also includes the charge exchange between electrons and oxygen ions, which can be described as the absorption O_2 obtaining electrons to create O^{2-} on the cathode surface. This process can be expressed as Eq. (2):

$$\frac{1}{2}O_2(\text{adsorbed}) + 2e^- \rightarrow O^{2-} \quad (2)$$

The low-frequency arc (right arc) is mainly attributed to oxygen adsorption or dissociation on the cathode surface and diffusion

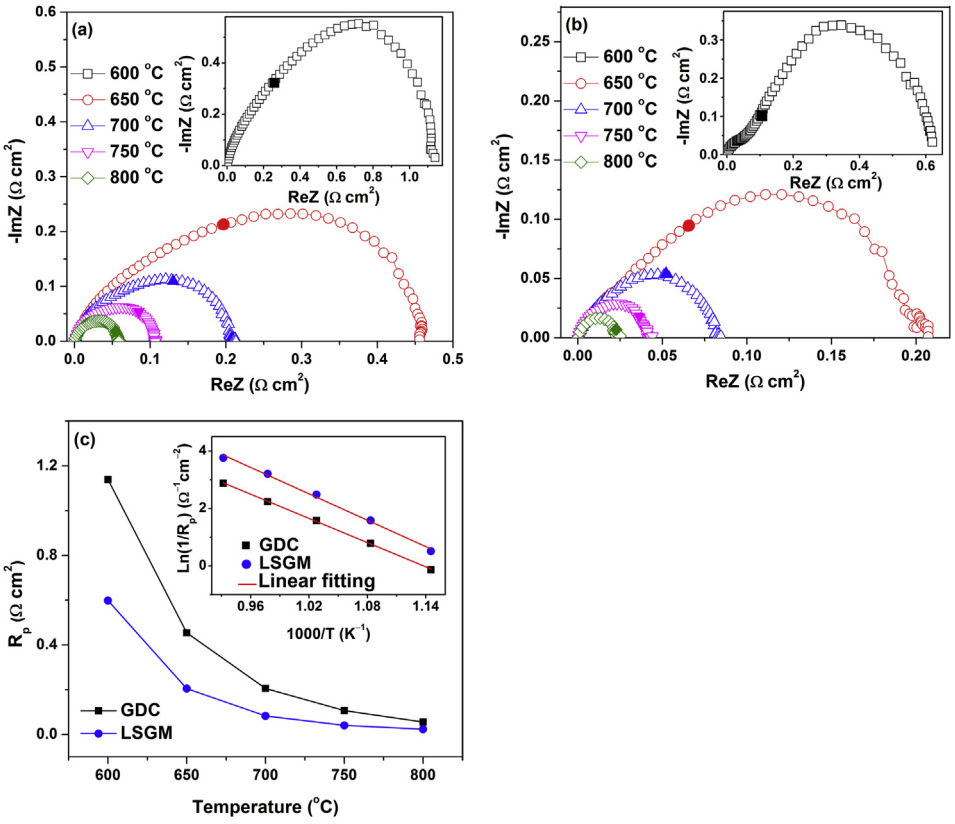

Fig. 7. Typical impedance of NBCFC cathode on (a) GDC and (b) LSGM electrolytes calcined at 950 °C for 2 h; (c) ASR of NBCFC cathode on GDC and LSGM electrolytes measured at 600 °C–800 °C. Inset shows the Arrhenius plots of the NBCFC cathode. The solid symbols in (a) and (b) indicate the frequency value of 1×10^2 Hz.

through the cathode bulk [35]. As shown in Fig. 7, the ASR values are significantly reduced with increasing temperature. The measured ASR values of the NBCFC cathode with the GDC electrolyte are 0.056, 0.107, 0.206, 0.455, and 1.139 Ω cm^2 at 800, 750, 700, 650, and 600 °C, respectively. Meanwhile, the ASR values of the NBCFC cathode with the LSGM electrolyte are 0.023, 0.041, 0.083, 0.205, and 0.599 Ω cm^2 at 800, 750, 700, 650, and 600 °C, respectively. Fig. 7(c) compares the ASR values of the NBCFC cathode with the GDC and LSGM electrolyte at different temperatures. We can see that the NBCFC cathode with GDC electrolyte shows larger ARS values than those with LSGM electrolyte, suggesting that the NBCFC cathode with LSGM electrolyte displays better electrochemical performance. This result may be because the LSGM electrolyte possesses higher ionic conductivity than the GDC electrolyte above 600 °C [1], which is useful in improving oxygen ionic transfer and diffusion. These ASR values in this study are substantially lower than that of the $GdBaCuCo_{0.5}Fe_{0.5}O_{5+\delta}$ double perovskite cathode with GDC electrolyte (1.409 Ω cm^2 at 700 °C) [17]. In particular, the ASR values of the NBCFC cathode with the LSGM electrolyte is lower than those of PBCFC, SBCFC, and GBCFC cathodes with GDC electrolyte, which are 0.144, 0.184, and 0.165 Ω cm^2, respectively, at 700 °C [15,16,18]. This value is also lower than the desirable target value of 0.150 Ω cm^2 at 700 °C as a cathode for IT-SOFCs [36]. The inset in Fig. 7(c) shows the Arrhenius plots of ASR values for the NBCFC cathode with GDC and LSGM electrolytes. The activation energies calculated for the oxygen reduction process on GDC and LSGM electrolytes are 116.8 and 127.3 kJ mol^{-1}, respectively. These activation energy values are lower or comparable to that of the PBCFC cathode with GDC electrolyte (118.9 kJ mol^{-1}) [18]. These results indicate that NBCFC is a highly advantageous cathode material for use in IT-SOFCs.

Fig. 8 shows the typical impedance spectra of NBCFC–GDC composite cathodes on the LSGM electrolyte. Moderate introduction of an electrolyte with high ionic conductivity into the electrode material can generally improve the oxygen diffusion rates and charge transfer of oxygen ions at the electrolyte/electrode interface, thus leading to enhanced electrochemical performance. However, the introduction of excessive ionic conductivity material in the

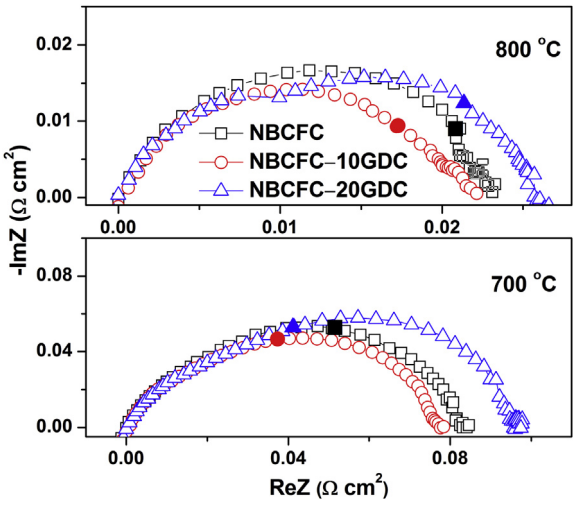

Fig. 8. Typical impedance of the NBCFC cathode and NBCFC–GDC composite cathodes on the LSGM electrolyte measured at 700 °C and 800 °C. Ohmic resistance was subtracted from the experimental data. The solid symbols indicate frequency value of 1×10^2 Hz.

composite cathode can hinder electronic conduction and cause inferior current collection, consequently leading to an increased ASR of the composite cathode. Therefore, the effects of electrolyte content on the electrochemical performance of composite cathodes are attributed to a consequence of competition between the two factors. As can be seen in Fig. 8, the ASR values decrease from 0.083 Ω cm^2 for NBCFC cathode to 0.077 Ω cm^2 for NBCFC–10GDC composite cathodes at 700 °C. The ASR of the NBCFC–10GDC composite cathode is lower than that of the NBCFC cathode at the same temperature, which indicates that the introduction of GDC enhances the electrocatalytic properties of the cathode, thereby reducing the ASR of the symmetric cell. Similar results have been reported for $LnBaCo_2O_{5+\delta}$–SDC composite cathodes [37]. However, ASR value increases as GDC content is further increased from 10 wt.% to 20 wt.%. This phenomenon can be explained by the non-continuous path of the electronic conduction caused by GDC particles in this composite cathode, leading to increased ASR. Regardless, the ASR of the NBCFC–20GDC composite cathode on LSGM is lower than the value of NBCFC on the GDC electrolyte and the desirable target value of 0.150 Ω cm^2 at 700 °C [36]. Therefore, considering the excellent electrochemical performance and decreased TEC, the NBCFC–*x*GDC composite cathodes are suitable for use in IT-SOFCs.

3.7. Single cell performance

The performances of electrolyte-supported Ni–GDC/GDC/NBCFC, Ni–GDC/GDC/LSGM/NBCFC, and Ni–GDC/GDC/LSGM/NBCFC–*x*GDC single cells were tested using dry hydrogen as fuel and ambient air as oxidant. Fig. 9 shows the cell voltage and power density as a function of current density for cells. In

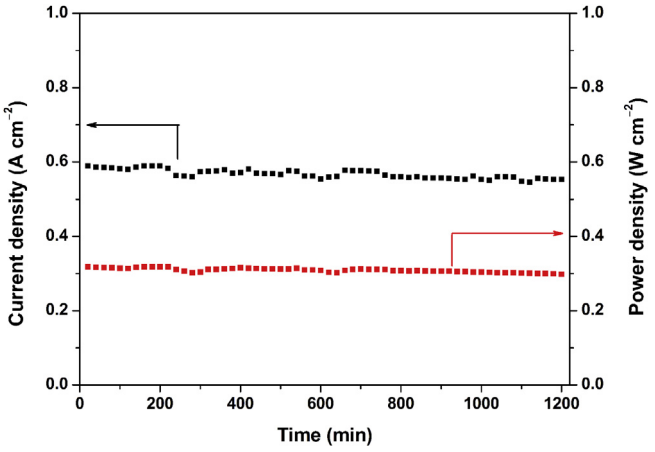

Fig. 10. Electrochemical stability of NBCFC cathode for Ni–GDC/GDC/LSGM/NBCFC cell at 700 °C.

Fig. 9(a), the maximum power density of the GDC-supported cell with the NBCFC cathode is 535 mW cm^{-2} at 800 °C. In Fig. 9(b)–(d), the maximum power densities of LSGM-supported cells with the NBCFC cathode, NBCFC–10GDC, and NBCFC–20GDC composite cathodes are 719, 736, and 654 mW cm^{-2} at 800 °C, respectively. The NBCFC–10GDC composite cathode shows the highest cell performance in comparison with NBCFC and NBCFC–20GDC cathodes. These results are in accordance with the impedance spectroscopy data in Figs. 7 and 8. The power density of the cell with LSGM electrolyte is higher than that with GDC electrolyte. This result can be

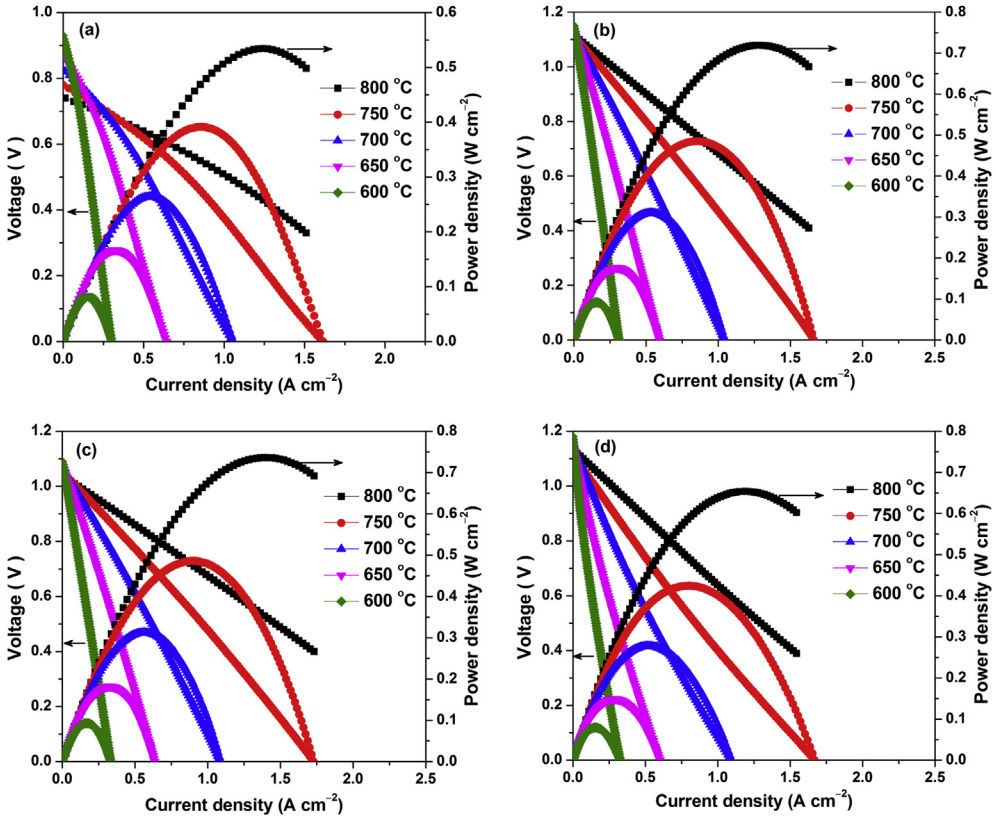

Fig. 9. Cell voltage and power density as a function of current density for electrolyte-supported cells with dry H_2 as fuel and ambient air as oxidant: (a) Ni–GDC/GDC/NBCFC, (b) Ni–GDC/GDC/LSGM/NBCFC, (c) Ni–GDC/GDC/LSGM/NBCFC–10GDC, and (d) Ni–GDC/GDC/LSGM/NBCFC–20GDC.

attributed to the higher ionic conductivity and stability under reducing conditions of the LSGM electrolyte than GDC at temperatures above 600 °C [1]. Notably, a lower open-circuit voltage is observed for GDC electrolyte-supported cell because of the partial reduction of Ce^{4+} to Ce^{3+} in the GDC electrolyte under an anodic atmosphere, which results in the short circuit of the internal electron conduction in GDC. The power density of the LSGM-supported cell using NBCFC as cathode is higher than that of the GDC-supported cell using PBCFC as cathode [18]. Fig. 10 shows the current density and power density of the cell with NBCFC cathode as functions of testing time at 700 °C fed with pure H_2. No significant degeneration of cell performance is observed within the 20 h testing duration. The preliminary result indicates that the NBCFC cathode has a good electrochemical stability. Therefore, the NBCFC and its composites are promising cathode materials for IT-SOFCs in terms of cell performance.

4. Conclusions

Pure near-stoichiometric NBCFC double perovskite with homogeneous grain size distribution was successfully prepared using an EDTA–citric acid complexation method. The structure and properties of NBCFC as a novel cathode material for IT-SOFCs with CeO_2- and $LaGaO_3$-based electrolytes were investigated. The NBCFC material obtained after sintering at 950 °C for 10 h crystallized in a tetragonal structure with the space group P4/*mmm*. XPS analyses revealed that Co^{3+}/Co^{4+}, Fe^{3+}/Fe^{4+}, and Cu^{+}/Cu^{2+} coexisted in the NBCFC, performing important functions in the conduction and electrochemical performance of the NBCFC cathode. Substitution of Fe and Cu for Co sites significantly reduced the TEC of the NBCFC cathode. The average TEC was 15.7×10^{-6} K^{-1} within the temperature range of 30 °C–850 °C. The electrical properties of the NBCFC material underwent a transition from a *p*-type semiconductor to metallically conductive behaviors at 625 °C, and the electrical conductivity reached a maximum of 92 S cm^{-1} at this temperature. The introduction of Cu significantly improved the high-temperature phase stability of NBCFC. The NBCFC material presented good chemical compatibility with GDC and LSGM electrolytes at 950 °C for 10 h, but not for the SDC electrolyte. The NBCFC cathode displayed good electrochemical performance, in which the ASR values were 0.056 and 0.023 Ω cm^2 at 800 °C with GDC and LSGM electrolytes, respectively. In addition, the maximum power densities reached 534 and 719 mW cm^{-2} at 800 °C for GDC- and LSGM-supported single cells, respectively. The use of the NBCFC–10GDC composite cathode led to further reduction in TEC and an improvement in electrochemical performance, in which the TEC value was decreased to 14.8×10^{-6} K^{-1} between 30 and 850 °C, and the ASR and cell performance with the LSGM electrolyte were 0.022 Ω cm^2 and 736 mW cm^{-2} at 800 °C, respectively. These results indicated that NBCFC is a promising cathode material for application in IT-SOFCs based on GDC and LSGM electrolytes. The combination of the NBCFC cathode with LSGM electrolyte is preferred in view of the good chemical compatibility and excellent electrochemical performance of the two materials.

Acknowledgment

This work was supported by the Natural Science Foundation of China (no. 10974065) and Applied Basic Research Programs of Science and Technology Development of Jilin Province (no. 20130102011JC).

References

[1] A.J. Jacobson, Chem. Mater. 22 (2010) 660–674.
[2] D.J. Brett, A. Atkinson, N.P. Brandon, S.J. Skinner, Chem. Soc. Rev. 37 (2008) 1568–1578.
[3] A. Maignan, C. Martin, D. Pelloquin, N. Nguyen, B. Raveau, J. Solid State Chem. 142 (1999) 247–260.
[4] K. Zhang, L. Ge, R. Ran, Z.P. Shao, S.M. Liu, Acta Mater. 56 (2008) 4876–4889.
[5] Q.J. Zhou, F. Wang, Y. Shen, T.M. He, J. Power Sources 195 (2010) 2174–2181.
[6] J.H. Kim, A. Manthiram, J. Electrochem. Soc. 155 (2008) B385–B390.
[7] J.H. Kim, L. Mogni, F. Prado, A. Caneiro, J.A. Alonso, A. Manthiram, J. Electrochem. Soc. 156 (2009) B1375–B1382.
[8] H.T. Gu, H. Chen, L. Gao, Y.F. Zheng, X.F. Zhu, L.C. Guo, Int. J. Hydrogen Energy 34 (2009) 2416–2420.
[9] V.A. Cherepanov, T.V. Aksenova, L.Y. Gavrilova, K.N. Mikhaleva, Solid State Ionics 188 (2011) 53–57.
[10] L. Zhao, B.B. He, Z.Q. Xun, H. Wang, R.R. Peng, G.Y. Meng, X.Q. Liu, Int. J. Hydrogen Energy 35 (2010) 753–756.
[11] Y.N. Kim, A. Manthiram, J. Electrochem. Soc. 158 (2011) B276–B282.
[12] Y.N. Kim, J.H. Kim, A. Manthiram, J. Power Sources 195 (2010) 6411–6419.
[13] J.H. Kim, A. Manthiram, Electrochim. Acta 54 (2009) 7551–7557.
[14] X.L. Che, Y. Shen, H. Li, T.M. He, J. Power Sources 222 (2013) 288–293.
[15] S.H. Jo, P. Muralidharan, D.K. Kim, Electrochem. Commun. 11 (2009) 2085–2088.
[16] S.J. Lee, D.S. Kim, P. Muralidharan, S.H. Jo, D.K. Kim, J. Power Sources 196 (2011) 3095–3098.
[17] Q.J. Zhou, T. Wei, S.Q. Guo, X.L. Qi, R.F. Ruan, Y. Li, Y. Wu, Q. Liu, Ceram. Int. 38 (2012) 2899–2903.
[18] F.J. Jin, S. Yu, R. Wang, T.M. He, J. Power Sources 234 (2013) 244–251.
[19] K.T. Lee, A. Manthiram, Chem. Mater. 18 (2006) 1621–1626.
[20] Y. Shen, M.N. Liu, T.M. He, S.P. Jiang, J. Power Sources 195 (2010) 977–983.
[21] F.J. Jin, H.W. Xu, W. Long, Y. Shen, T.M. He, J. Power Sources 243 (2013) 10–18.
[22] L.G. Cong, T.M. He, Y. Ji, P.F. Guan, Y.L. Huang, W.H. Su, J. Alloy Compd. 348 (2003) 325–331.
[23] R.D. Shannon, Acta Cryst. A32 (1976) 751–767.
[24] M. Ghaffari, M. Shannon, H. Hui, O.K. Tan, A. Irannejad, Surf. Sci. 606 (2012) 670–677.
[25] P. Bera, K.R. Priolkar, P.R. Sarode, M.S. Hegde, S. Emura, R. Kumashiro, N.P. Lalla, Chem. Mater. 14 (2002) 3591–3601.
[26] A. Kopia, K. Kowalski, M. Chmielowska, C. Leroux, Surf. Sci. 602 (2008) 1313–1321.
[27] M.A. Señarís-Rodríguez, J.B. Goodenough, J. Solid State Chem. 118 (1995) 323–336.
[28] I.D. Brown, R.D. Shannon, Acta Cryst. A29 (1973) 266–282.
[29] G.K. Zhang, L.Q. Qin, Mater. Chem. Phys. 74 (2002) 324–327.
[30] B. Wei, Z. Lu, S.Y. Li, Y.Q. Liu, K.Y. Liu, W.H. Su, Electrochem. Solid-State Lett. 8 (2005) A428–A431.
[31] A.I. Klyndyuk, E.A. Chizhova, Glass Phys. Chem. 40 (2014) 124–128.
[32] K. Gaur, S.C. Verma, H.B. Lal, J. Mater. Sci. 23 (1988) 1725–1728.
[33] L.W. Tai, M.M. Nasrallah, H.U. Anderson, D.M. Sparlin, S.R. Sehlin, Solid State Ionics 76 (1995) 273–283.
[34] Q.J. Zhou, Y.C. Zhang, Y. Shen, T.M. He, J. Electrochem. Soc. 157 (2010) B628–B632.
[35] Y. Shen, F. Wang, X. Ma, T. He, J. Power Sources 196 (2011) 7420–7425.
[36] B.C.H. Steele, Solid State Ionics 86–88 (1996) 1223–1234.
[37] D.J. Chen, R. Ran, Z.P. Shao, J. Power Sources 195 (2010) 7187–7195.